JEM

SUPPLEMENTAL MATERIAL

Séror et al., http://www.jem.org/cgi/content/full/jem.20101805/DC1

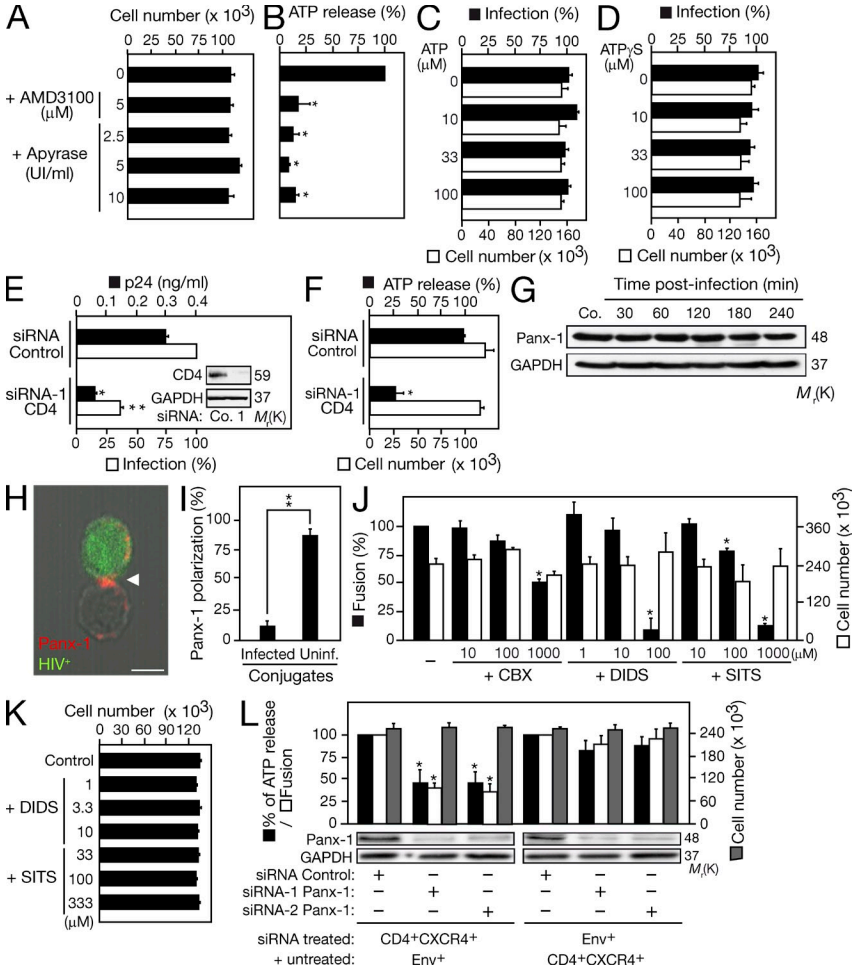

Figure S1. Pannexin-1–dependent ATP release during HIV-1 infection and during HIV-1 Env-mediated fusion. (A) CD4+CXCR4+ cells expressing a Tat-inducible β-gal reporter gene were infected with HIV_{NL43} (MOI = 1) in the presence of 5 µM AMD3100 and of different concentrations of apyrase. Target cell viability was evaluated by determining the absolute number of total live cells after incubation for 3 h with different concentrations of apyrase or AMD3100 (as indicated) and after infection with $HIV\text{-}1_{NL43}$ for 2 d (mean ± SEM; $n = 3$). Note that the initial number of cell was 1–2 × 10^4 cells per well. (B) CD4+CXCR4+ cells were infected with HIV_{NL43} (MOI = 1) in the absence or in the presence of 2.5, 5, or 10 UI/ml apyrase or 5 µM AMD3100. After 2 h of infection, ATP release was determined (mean ± SEM; *, $P < 0.01$; $n = 3$). (C and D) CD4+CXCR4+ cells expressing a Tat-inducible β-gal reporter gene were infected with HIV_{NL43} (MOI = 1) in the absence or in the presence of 10, 33, or 100 µM ATP or ATP-γS. After 2 d of infection, host cell infectivity and viability were assessed as described (means ± SEM; $n = 3$). (E and F) CD4+CXCR4+ cells expressing a Tat-inducible β-gal reporter gene were transfected with siRNA specific for CD4 or control siRNA and were infected with HIV_{NL43} (MOI = 1) during 2 d. Then, viral production (E), host cell infectivity (E), ATP release (F), and target cell viability (F) were determined (means ± SEM; $n = 3$; *, $P < 0.01$; **, $P < 0.001$). Depletion of CD4 was assessed by immunoblot, and GAPDH expression was determined as loading control (inset in E). (G) Primary lymphoblasts were infected with HIV_{NDK} (MOI = 1) for the indicated periods. Pannexin-1 expression was determined by immunoblot. Representative immunoblots of three independent experiments are shown. (H) Subcellular localization of pannexin-1 (red) during the interaction between HIV-1–infected lymphoblasts (green) and uninfected lymphoblasts was assessed by immunofluorescence microscopy. One representative image for four independent experiments is shown (bar, 5 µm). (I) Frequency of Panx-1 polarization in HIV-1–infected and uninfected cells during cell conjugate formation (mean± SEM; $n = 3$; **, $P < 0.001$). (J) Fusion between 1.2 × 10^5 HIV-1 Env+ cells (that also express Tat protein) and 1.2 × 10^5 CD4+CXCR4+ target cells (that contain Tat-inducible β-galactosidase) in the absence or presence of indicated concentrations of pannexin-1 pharmacological inhibitors, CBX, DIDS, and SITS was determined by measuring β-galactosidase (β-Gal) activity 24 h after co-culture (mean ± SEM; $n = 3$; *, $P < 0.05$). Cell viability was assessed as in A. (K) CD4+CXCR4+ HeLa cells (initially 1–2 × 10^4 cells per well) were infected with HIV_{NL43} (MOI=1). Target cell viability was determined 3 d after infection (mean ± SEM; $n = 3$). (L) Env+ or CD4+CXCR4+ HeLa cells depleted of pannexin-1 were cocultured with their fusion partners for 24 h. Then HIV-1 Env–mediated fusion was evaluated as described (mean ± SEM; $n = 3$; *, $P < 0.01$). The knockdown of pannexin-1 by two nonoverlapping siRNAs was confirmed by immunoblotting. The number of total viable cells after pannexin-1 depletion was assessed, as in J, 24 h after co-culture (mean ± SEM; $n = 3$).

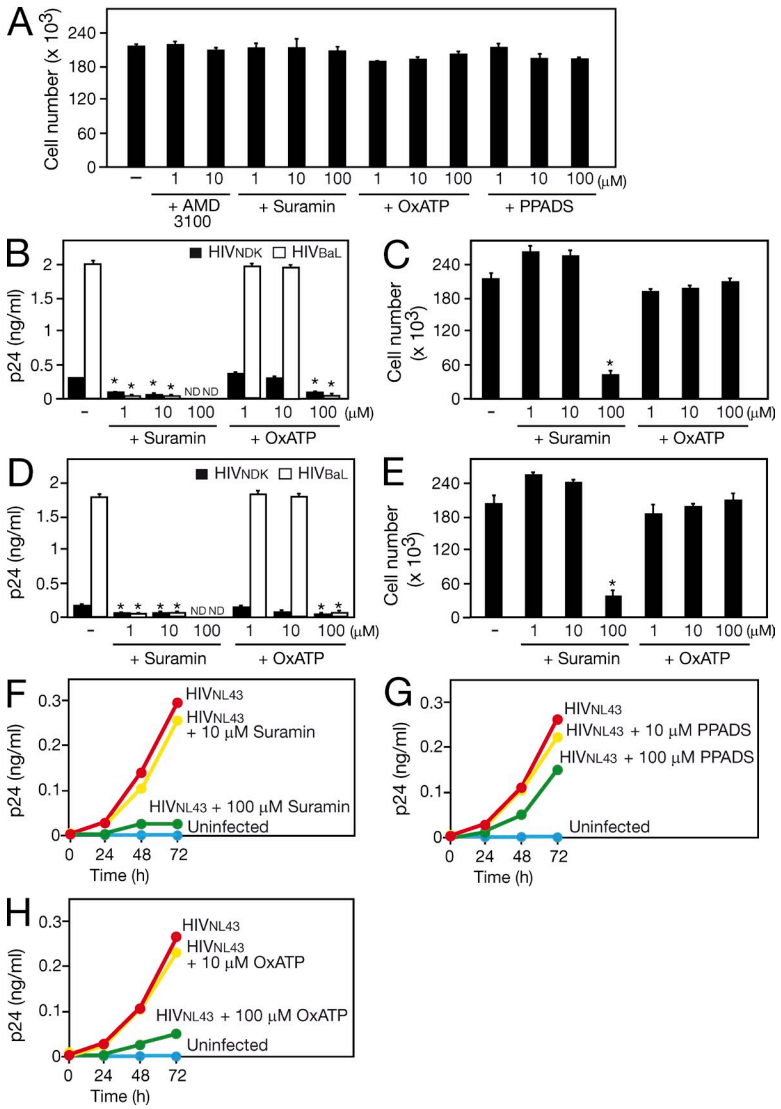

Figure S2. Impact of P2 inhibitors on cell viability, viral production, host cell infectivity, and hemifusion/fusion during HIV infection. (A–E) Primary human lymphoblasts (A), human MDM (B and C), and human MDDCs (D and E) were infected with X4-tropic (HIV-1_{NDK}) or R5-tropic (HIV-1_{BaL}) HIV-1 strains (MOI = 1) for 3 d in the presence or absence of the indicated concentrations of the P2 receptor antagonist suramin, the P2X-selective antagonist OxATP, or the P2Y-selective antagonist PPADS. The total number of live cells was evaluated 3 d after infection. Results were obtained from three independent experiments (mean ± SEM; *, $P < 0.05$). (F–H) C8166 T cells were infected with clinical isolates (MOI = 1). p24 was measured by means of an ELISA 24, 48, or 72 h after infection in the presence of the indicated concentrations of the P2 receptor antagonist suramin (F), the P2Y-selective antagonist PPADS (G), or the P2X-selective antagonist OxATP (H). The results are representative of three independent experiments.

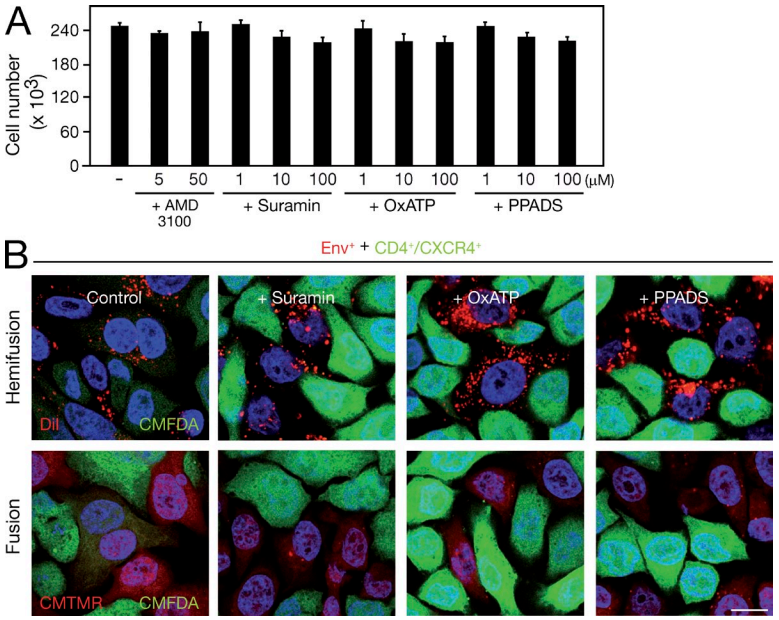

Figure S3. Effects of CXCR4 antagonist AMD3100 and P2 inhibitors on co-cultured Env⁺ and CD4⁺CXCR4⁺ HeLa cells. (A) Absolute number of total live cells was determined in the absence or presence of the indicated concentrations of AMD3100, suramin, PPADS, or OxATP after 24 h of co-culture. Results are means ± SEM of three independent experiments. (B) Effects of 5 µM AMD3100, 10 µM suramin, 100 µM PPADS, and 100 µM OxATP on hemifusion and fusion mediated by HIV-1 envelope were determined. Representative micrographs of three independent experiments are shown. The quantitation of these results is shown in Fig. 2 C (bar, 5 µm).

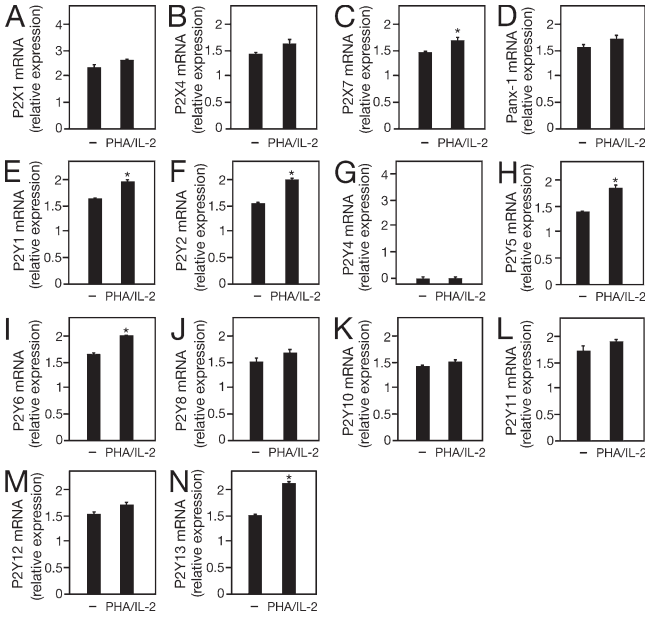

Figure S4. Purinergic receptor and pannexin-1 expression on human PBMCs and PHA/IL-2–stimulated PBMC. (A–N) P2X1, P2X4, P2X7, Panx-1, P2Y1, P2Y2, P2Y4, P2Y5, P2Y6, P2Y8, P2Y10, P2Y11, P2Y12, and P2Y13 mRNA expression in human PBMC and on PHA⁺IL-2–stimulated PBMC were measured by quantitative real time RT-PCR. Data were pooled from three independent experiments (mean ± SEM; *, $P < 0.001$).

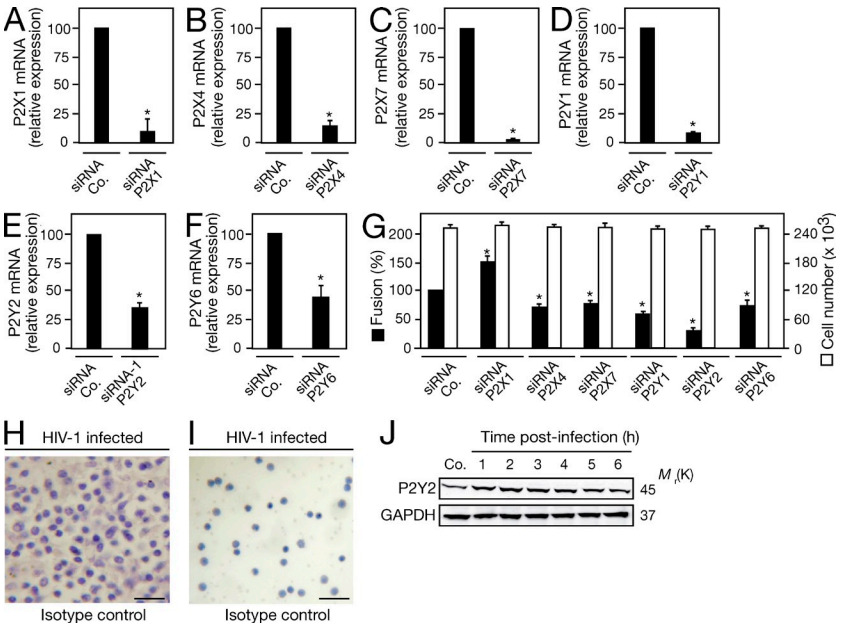

Figure S5. Identification of purinergic receptors involved in HIV-1 Env–mediated fusion and controls for immunohistochemical analyses. (A–F) $CD4^+CXCR4^+$ cells were transfected during 48 h with specific siRNA for P2X1, P2X4, P2X7, P2Y1, P2Y2, P2Y6, or control siRNA. Reduction of the corresponding mRNAs was estimated by means of quantitative real time RT-PCR. Error bars indicate SEM of duplicate determinations. *, $P < 0.01$. (G) Cell fusion mediated by HIV-1 envelope was evaluated by determining β-Gal activity during co-culture with HIV-1 Env^+ cells. Error bars in G represent SEM of triplicate determinations. *, $P < 0.05$. The absolute number of total live cells was also determined during experiments. (H and I) Representative immunochemistries of lymph nodes (H) and PBMC (I) from HIV-1–infected patients obtained after incubation with an isotype control antibody (bars, 50 µm) are shown. (J) $CD4^+CXCR4^+$ cells were infected with HIV-1_{NL43} (MOI = 1) for the indicated periods. P2Y2 expression was determined by immunoblot. Representative immunoblots of three independent experiments are shown.

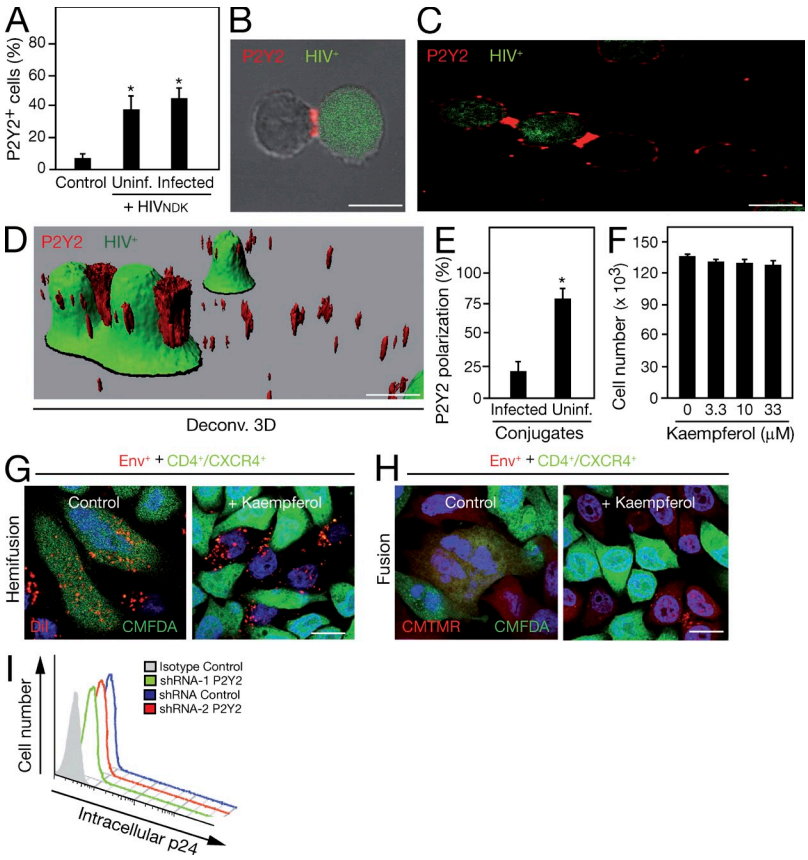

Figure S6. Detection of polarized P2Y2 at the virological synapse mediated by HIV_{NDK}. (A) Human lymphoblasts were infected for 3 d with HIV_{NDK} (MOI = 1), stained with 10 µM 5-chloromethylfluorescein diacetate (Cell Tracker green; CMFDA) and cocultured with uninfected lymphoblasts. Then, P2Y2 overexpression was assessed by fluorescence microscopy, and the frequency of cells that overexpress P2Y2 was determined among the HIV-1–infected versus uninfected cells (mean ± SEM; $n = 3$; *, $P < 0.001$). (B and C) P2Y2 polarization (in red) between HIV-1–infected lymphoblasts (in green) and uninfected lymphoblasts (B and C), and among interacting HIV-1–infected lymphoblasts, was analyzed by confocal microscopy. Representative micrographs of four independent experiments are shown. (D) 3D reconstruction of merged images (representative of three independent experiments) was performed. (E) Lymphoblasts were infected, stained, and cocultured with uninfected lymphoblasts. After 48 h of co-culture of HIV-1–infected CMFDA-stained lymphoblasts with uninfected lymphoblasts, the polarization of P2Y2 was evaluated. The frequency of P2Y2 polarization in HIV-1–infected and uninfected cells that formed mixed conjugates was determined (mean ± SEM; $n = 3$; *, $P < 0.001$). (F) 15 thousand $CD4^+CXCR4^+$ HeLa cells were infected with HIV-1NL43 for 2 d in the presence of the indicated concentrations of the kaempferol and the total number of viable cells was determined (mean ± SEM; $n = 3$). (G and H) HeLa Env^+ and HeLa $CD4^+CXCR4^+$ cells were, respectively, stained for hemifusion analysis with $DiIC_{18}(3)$ and with CMFDA or were stained for cell–cell fusion analysis, respectively, with CMFDA and with CMTMR. Then, cells were cultured together for 24 h in the presence of 33 µM of P2Y2 receptor antagonist kaempferol. Representative micrographs of three independent experiments are shown. Bars, 5 µm. (I) Representative flow cytometric analysis of intracellular p24 antigen in uninfected T CEM cells transduced with lentiviruses encoding shRNA constructs. Representative profiles of three independent experiments are shown.

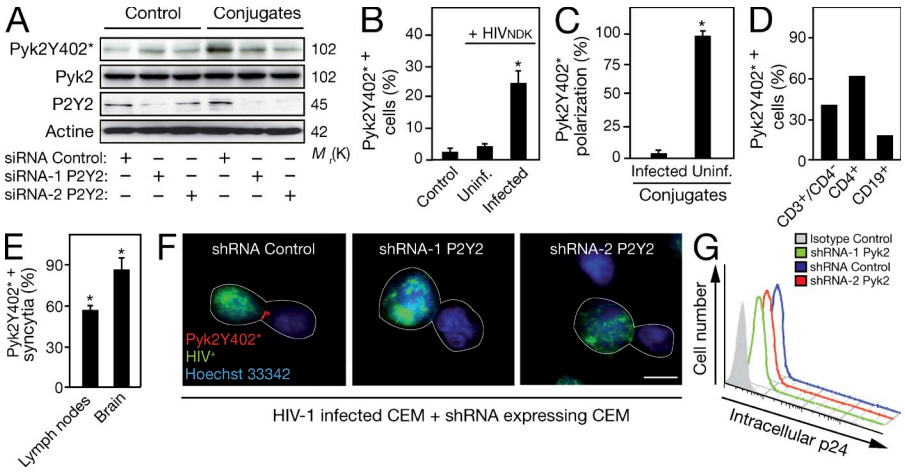

Figure S7. Activation of Pyk2 during HIV-1 infection. (A) CD4+CXCR4+ HeLa cells were transfected during 48 h with siRNAs specific for P2Y2 or control siRNA and cocultured with Env+ HeLa cells. After 6 h of conjugate formation, Pyk2Y402* and Pyk2 expression were determined by immunoblotting. Actin expression was determined as a loading control. The blot is representative for three independent experiments. (B) Human lymphoblasts were infected for 3 d with HIV_{NDK} (MOI = 1), stained with 10 µM of 5-chloromethylfluorescein diacetate (Cell Tracker green; CMFDA) and cocultured with uninfected lymphoblasts. Then, cells that are positive for Pyk2Y402* were evaluated by immunofluorescence microscopy, and the frequency of Pyk2Y402*-positive (Pyk2Y402*+) cells in HIV-1–infected cells and in uninfected cells was determined (mean ± SEM; $n = 3$; *, $P < 0.001$). (C) The frequency of Pyk2Y402* polarization in HIV-1–infected and in uninfected cells that formed mixed conjugates was determined (mean ± SEM; $n = 3$; *, $P < 0.001$). (D) PHA+IL-2–stimulated human PBMCs were infected during 6 d with HIV_{NDK}. Then the frequency of Pyk2Y402*+ cells was determined among $CD3^+CD4^-$ cells, $CD4^+$, cells and $CD19^+$ by three-color immunofluorescence and flow cytometry. One representative experiment out of three is shown. (E) Immunohistochemical detection of Pyk2Y402* in lymph node biopsies and frontal cortex biopsies from infected patients was realized and frequency of Pyk2Y402*-positive (Pyk2Y402*+) syncytia was determined (mean ± SEM; $n = 5$; *, $P < 0.01$). (F) HIV_{NDK}-infected CEM cells were incubated during 6 h with uninfected CEM cells previously transduced with indicated lentiviruses encoding shRNA constructs. Frequency of Pyk2Y402* polarization at the contact site between conjugates formed was analyzed. Representative micrographs of three independent experiments are shown (bar, 5 µm). These results have been quantitated in (Fig. 6 M). (G) Representative flow cytometric profiles of intracellular p24 antigen in uninfected T CEM cells that were depleted or not for Pyk2. Results shown are representative of three independent experiments.